CrossMark

RESEARCH PAPER

Pattern recognition of seismogenic nodes using Kohonen self-organizing map: example in west and south west of Alborz region in Iran

Mostafa Allamehzadeh · Soma Durudi · Leila Mahshadnia

Abstract Pattern recognition of seismic and morphostructural nodes plays an important role in seismic hazard assessment. This is a known fact in seismology that tectonic nodes are prone areas to large earthquake and have this potential. They are identified by morphostructural analysis. In this study, the Alborz region has considered as studied case and locations of future events are forecast based on Kohonen Self-Organized Neural Network. It has been shown how it can predict the location of earthquake, and identifies seismogenic nodes which are prone to earthquake of $M5.5+$ at the West of Alborz in Iran by using International Institute Earthquake Engineering and Seismology earthquake catalogs data. First, the main faults and tectonic lineaments have been identified based on MZ (land zoning method) method. After that, by using pattern recognition, we generalized past recorded events to future in order to show the region of probable future earthquakes. In other word, hazardous nodes have determined among all nodes by new catalog generated Self-organizing feature maps (SOFM). Our input data are extracted from catalog, consists longitude and latitude of past event between 1980–2015 with magnitude larger or equal to 4.5. It has concluded node D1 is candidate for big earthquakes in comparison with other nodes and other nodes are in lower levels of this potential.

M. Allamehzadeh · S. Durudi (✉) · L. Mahshadnia
Seismology Department, International Institute of Earthquake Engineering and Seismology, IIEES, Tehran, Islamic Republic of Iran
e-mail: somdr@ymail.com

M. Allamehzadeh
e-mail: zadeh66@hotmail.com

L. Mahshadnia
e-mail: l.mahshadnia@iiees.ac.ir

1 Introduction

The Alborz mountain range is part of the northern boundary between Iran and Eurasia, located South of the Caspian sea. Historical background and instrumentally located earthquakes as well as the geological evidences all show that Alborz region is one of the seismically active regions in the Middle East (Gheitanchi et al. 2006). One of the largest shocks (M_S 7.7) has occurred on 20 June 1990, in the West of Alborz. Nearly 40,000 people were killed, and more than 500,000 lost their homes (Berberian and Walker 2010). The damage was substantial and spread over a widely populated area.

Such as this destructive earthquakes in the world motivate to develop the systematic and testable assessments capable of providing consistent information about the sites where large earthquakes may occur. This is highly important for knowledgeable seismic hazard evaluation. Forecasting earthquake has been faced as a great challenge in seismology more than 100 years (Geller 1997).

Despite the great effort made and the multiple models developed by different authors (Tiampo and Shcherbakov 2012), no successful method has been found yet. Due to the random behavior of earthquakes generation, it may never be possible to ascertain the exact time, magnitude and location of the next damaging earthquake (Reyes et al. 2012).

Regional seismicity has usually been disturbed before large earthquakes, so that, small earthquakes occurred few months before the main shock in the area that their

Springer

epicenters seem to be completely random but they follow some particular patterns or shapes. Spatial prediction of these earthquakes is complicated, but it is possible by using advanced statistical methods nowadays.

Many authors have proposed different methods to predict the occurrence of earthquakes. The work in Ward (2007) added five different models to the Regional Earthquake Likelihood Model (RELM). The first one model presented by Kagan et al. (2007) was based on smoothed seismicity and predicted earthquakes with magnitude greater or equal to 5.0. The second model is similar to the one proposed by Jackson et al. (2009). The third is based on fault data analysis. The fourth model is a combination of the first three models and, finally, the last one is based on earthquake simulations (Ward 2000).

A related work was presented by Gorshkov et al. (2003). In this method, land zoning method (MZ) was used for identifying structural instability for determining the structure of faulting in the earthquake prone areas. MZ method is based on geomorphic and geological data and does not rely on the knowledge about past seismicity (Alexeevskaya et al. 1977). The fact that earthquakes nucleate at nodes was first established for the Pamirs and Tien Shan regions (Gelfand et al. 1972). This is basic assumption to identify area prone earthquake. The roles of intersecting faults are observed in different tectonic settings. Talwani (1988) found that large intraplate earthquakes were related to intersections and demonstrated by intersecting faults providing a location for stress accumulation (Gorshkov et al. 2009). This method has been tested in many seismicity parts of the world, and the results have been confirmed by occurring extreme events in the areas where they had been studied before, so that 87% of seismic events occurred at the nodes that are delineated around the intersections of lineament (Soloviev et al. 2014). This amount proves the reliability and statistical significance of the approach.

The pattern recognition technique has employed to select among all the nodes those, which are prone to earthquakes above a certain (target) magnitude. The first application of pattern recognition was introduced by Gelfand et al. 1970. Since the early 1970s, the methodology has been successfully applied in a number of regions worldwide, including California, where it permitted the identification of earthquake prone areas that have been subsequently struck by strong events and that previously were not considered seismogenic (see the overviews by Gorshkov et al. 2003; Soloviev et al. 2014).

The morphostructural analysis has been already applied to the Italian mountain ranges, namely in the Alps (Gorshkov et al. 2004) and in peninsular Italy and Sicily (Gorshkov et al. 2002), and also in Alborz region (Gorshkov et al. 2009). The feasibility of such analysis (MZP) has been established for topographically flat basins within

Iberian Peninsula (Gorshkov et al. 2010) and recently for the Rhone valley in France (Gorshkov and Gaudemer 2012).

A formal identification of priority areas, most prone to future seismic activation, can be performed integrating the space information provided by the earthquake prone areas with the spacetime information provided by formally defined earthquakes predictions (e.g., Peresan et al. 2011). A number of forecasting methodologies have been developed, mainly based on the analysis of seismicity, and are currently applied both at national and international scale (Jordan et al. 2011).

2 Geological and tectonic features

The active belt of seismicity in northern Iran coincides with the Alborz mountains. The occurrence of moderate to large earthquakes in the Alborz implies the significance of current tectonic deformation taking place on this mountain belt (Zolfaghari 2008).

The studied area extends from 48°E to 51°E in longitudes and from 35°N to 38°N in latitudes. The region extended in Alborz, part of Central Iran and Sanandaj-Sirjan geological zones. The Alborz mountains, forming a gently sinuous East-West range across northern Iran south of the Caspian sea, constitute a northern part of the Alpine-Himalayan orogeny in western Asia. They face the Caspian block on the north and to the south grade into the plateau of Central Iran. In its western part, the range shows NW–SE, trending structures, roughly parallel to the northern part of the Zagros seismic zone and to the structural alignments of Caucasus. The western and eastern Alborz, two different structural trends, meet each other in the Central Alborz. In the zone of convergence between these two different alignments, the great Quaternary volcano of Damavand is shaped (Gheitanchi et al. 2006). Geological evidence and fault plane solutions of earthquakes in Alborz region indicate the existence of both thrust and conjugate strike-slip faulting (Jackson 1992).

Several major faults with almost east-west trends in north and northeast Tehran, the Rudbar fault system in northwest, and the Ipak in west are examples of well-known major faults in Alborz region that have experienced destructive earthquakes in the past (Fig. 1).

Surrounding the south Caspian basin, the Alborz mountain range shows strong tectonic activity with several destructive earthquakes in the past (Berberian and Yeats 2001).

The South Caspian basin is an aseismic block in the Alpine belt which is surrounded by several zones of high seismic activity. The Talesh and Alborz mountains are
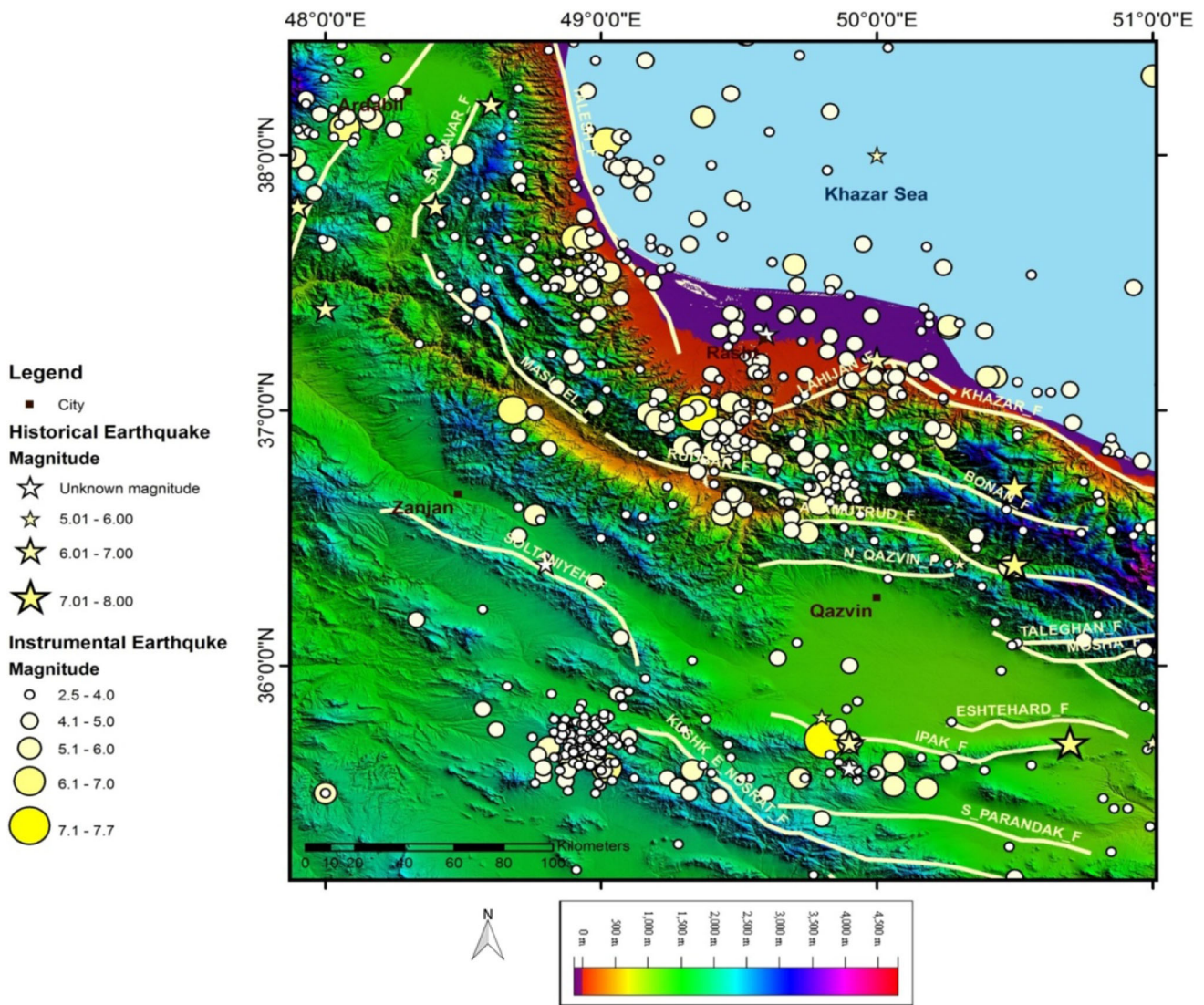
Fig. 1 Active faults and seismicity of the region under studied. These data has been recorded from 1900 to 2015

overthrusting the "oceanic-like crust" of the South Caspian basin (e.g., Berberian 1983).

The tectonic blocks and areas in the studied region, along northwest–southeast, from the northwest to the southeast, include: the active tectonic area of Talesh which is composed of several thrust faults with NW trends. Ghezel Ozan intramountain basin, in the form of a large syncline with fold axes which is parallel to NW, is located in the Southwest area of Talesh.

Tarom magmatic arc formed the North of the city of Zanjan and the Southern part of the Western Alborz in a mountainous shape. In this block, the faults that are parallel to mountain ranges are more active than other faults. Thrust ancient rock units on the Neocene units show the activity of these faults in the current era.

The border of the Alborz and Central Iran zones, as longitudinal lineament, passes from Qazvin plain, Zanjan,

and Abhar. The Southern regions in the Tarom mountains, part of the Central Iran zone, are divided into several tectonic blocks which limited to fault lineaments by the activity of faults with the trends of NW–SE. The most important ones are:

The tectonic subsidence basin of Zanjan-Abhar, as a shape of a narrow plain, covered by Quaternary alluvium, extends from Znajan to Abhar.

The Soltanieh Horst, as a narrow mountainous line with trend of NW–SE that is parallel to the Tarom mountains, extended from Zanjan to Abhar by the active fault of Soltanieh. This horst is the result of the activity of the southeast segment of Tabriz fault which is resulted of Pyrenean orogenic.

The intramountain subsidence of Ozon Dareh is a gentle synclinal basin which is filled by Cretaceous and Tertiary rocks, and young alluvium. This plain is parallel to the

Southwest segment margin of Soltanieh mountain. Lastly, Urumieh-Dokhtar zone is located in the middle of Sanandaj-Sirjan zone and Soltanieh Graben, and also, it is parallel to the both.

3 Methodology

The methodology involves two steps. The first is to identify objects of recognition using the method of morphostructural zoning, with the objects being nodes of intersections of morphostructural lineaments. The second step uses pattern recognition algorithms to find those intersections, where large earthquakes may occur.

3.1 Morphostructural zoning method

According to Keilis-Borok (1990), a hierarchical dynamic system of lithospheric blocks and their boundaries is the supporting medium of seismicity. Therefore, delineation of block and fault geometry for a seismic region is a necessary stage in studying earthquake prone areas. In order to delineate the block structure of the West and South Alborz, we employ the morphostructural zoning method.

The methodology used is based on the idea that large earthquakes nucleate at nodes, specific structures that are formed around the intersection of mobile boundary zones separating different blocks of the Earth's crust. In the framework of the methodology, nodes are delineated with morphostructural zoning method (Gorshkov et al. 2003).

The present-day topography of the study region is the main subject of the analysis in MZ. The study region is divided into a system of hierarchically ordered areas characterized by homogeneous present-day topography and tectonic structure. The blocks are assigned from the highest to lowest rank, by lineaments. Lower rank blocks are parts of a higher rank block. The block of a higher category is divided into two blocks, belonging to the below category. Usually, three levels of a hierarchy were considered in different regions. Blocks of the first rank, mountain countries, are divided into blocks of the second rank, megablocks. Megablocks are further divided into blocks of the third rank, called blocks. Lineaments themselves include types and varying degrees including: longitudinal and transverse ones.

Longitudinal lineaments are approximately parallel to the regional strike of the tectonic structure and the topography and, as a rule, include the prominent faults that separate mountainous regions from the areas which subsided comparatively or are subsidence basins. Transverse lineaments go across the regional trends of tectonic structure and topography. Normally, they appear on the Earth's surface discontinuously and are evidenced by escarpments,

rectilinear parts of river valleys, and partly by faults (Peresan et al. 2013).

One of the dependent parameters of the intensity of tectonic movements is the difference between maximum and minimum topographic height. These lineaments show high adaptation with the isostatic balance, elastic bending, and horizontal compressive forces in lithosphere (Snyder and Barazangi 1986).

The variations of the lithospheric thickness or density play an important role in creating lithospheric forces (England and McKenzie 1982; Assameur and Mareschal 1995). Large isostatic anomalies may exist in the areas where tectonic forces are active, therefore, the most important feature of the seismic activities determined by height, so the most seismicity areas overlaid on regions where topographic loading is big or the gradient of the gravity anomalies is high (Seeber et al. 1981; Keary and Vine 1996; Jackson and McKenzie 1984; Moores and Twiss 1995; Dalmayrac and Molnar 1981; Zamani and Hashemi 2000).

One of the dependent parameters of heterogeneity in the depth of crust is the difference between maximum and minimum gravity anomalies (relief anomaly). There are lineaments which are result of joining points with minimum distance of the difference between maximum and minimum anomalies contour. These anomalies are dependent of Gravity distribution such as isostatic anomaly. These lineaments can be a suitable index for determining the borders of the main lithospheric blocks with relative displacement and high seismicity potential (Gorshkov et al. 2003).

Therefore, structural lineaments are obtained from topographic lineaments, which are overlaid with rapid variation of isostatic anomalies. The variation of thickness and the distribution of block crust can cause stress systems with fault spreading potential and seismicity localization at the border of block (Bott and Dean 1972).

In this study, we identified fundamental faults and tectonic lineaments with the maximum gradient of gravity, magnetic, topography, isostasy anomalies, and also, we evaluated their correspondence together and satellite images. It has concluded that topographic lineaments have high adaptation with lineaments, obtained from other anomalies. These indexes indicate the variations of intensity tectonic movement, the degree of lithosphere disruption, and the heterogeneity of depth crust. The points at the intersections of these lineaments on the active faults have created the seismic nodes (Fig. 2).

Nogol Sadat (1978) has divided the longitudinal faults and structural lineaments of the Iran plateau, the boundaries of structural and sedimentary blocks, into three main categories: trends of N striking (formed in the late Precambrian and Katangai orogeny), NE striking (with left-
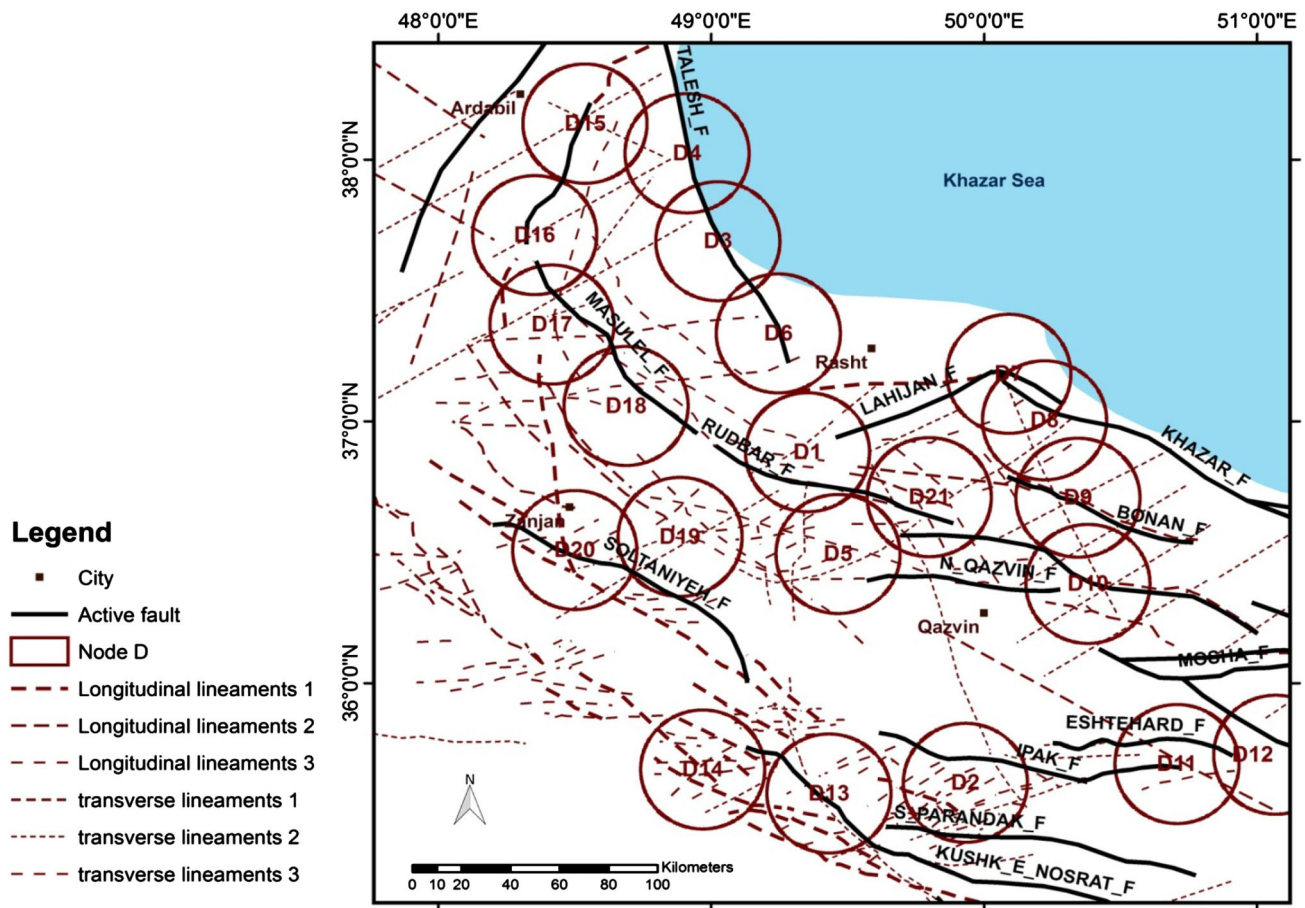
Fig. 2 Seismogenic nodes in Zanjan-Rudbar based on morphostructural zoning method (Hessami et.al. 2003)

lateral component as old as Devonian age), and NW trends (left-lateral faults that formed in the Late Precambrian and Katanga cycle). In addition, other faults with EW trends that deform Iran plateau are detectable in the topographic, magnetic, and gravity anomaly maps.

Morphostructural nodes are formed around the intersections of two or more lineaments. A node may include more than one intersection or junction. The size and geometry of a node can be outlined with fieldwork if the morphological field studies are not done for determining the ranges of nodes, it will consider as a certain circle and its extent is usually determined by the radius which is proportional to earthquake magnitude.

The specifications of the important seismic nodes in the study area are as follows (Fig. 2):

Node D1 The node is located at the intersection of Masouleh fault (the Northeast of the Qezel-Ozan valley) and the transverse lineaments which is the border of West and Central Alborz, and also the transverse lineaments parallel to Lahijan and Rudbar faults. Masouleh fault separates two large blocks from each other, which are different in heights and azimuths together, including Kopet

Dagh mountain (North-Northeast) and Anguran mountain (Southwest). The Transverse lineament with trend of NNW, at Southern sector of Talesh fault, separate the Western Alborz with high tectonic structure along East-West, and right-lateral displacement, from Central Alborz. As the result of this lineament in southern parts, the plain of Zanjan separates from the Southern basin of Qazvin.

The distribution of magnetic intensity at the location of this node demonstrates the existence of maximum magnetic changes along the transverse lineament with the trend of NE, and also along the Masouleh fault. Since considerable changes are not observed in lithology along the mentioned lineament, it can be stated that the magnetic changes in the North of Rudbar were affected from regional tectonic activity. The occurred quake on June 21, 1990, and its aftershocks at this node confirmed seismic importance of this node.

Node D2 This node is located at the South of Buin Zahra and at the intersection of Soltanieh- Parandak longitudinal lineament, Aypek fault, the Southern fault of Parandak, and the transverse lineaments with trends of NE and NW. Historical earthquakes in the range of this node include:

- An earthquake in the third millennium BC, at the border of the Qazvin plain and the Soltanieh block (49.9°E–35.6°N).
- The earthquake of 10th of December 1119 AD with magnitude of 6.5 in Qazvin plain (49.9°E–35.7°N).
- The earthquake of 20th of October 187 AD with magnitude of 5.7 at the border of the Qazvin plain and Zanjan (49.8°E–35.8°N).

Node D14 This node is located at the North of Razan at the intersection of the Kooshk-Nosrat fault, the border of the Central Iran and Sanandaj-Sirjan zones, and transverse lineament with trend of NE.

D3 and *D4* These nodes, the intersection of the transverse lineaments with trends of SE and NW, on the Talesh fault lead to obvious changes in the magnetic intensity along the fault. Such the position can be seen at the node D6 in the Southern Talesh fault with the difference that unlike the two nodes mentioned above, this node has no important historical or instrumental record. So, probably, it meets seismic quiescence condition.

D15 and *D16* These nodes are located at the intersections of the lineament NE-NW trending, along the Sangavar fault.

Node D20 This node is located at the East of Mahneshan and the intersection of the magnetic lineaments with the trend of N and Soltanieh and Zanjan faults and the northern–southern lineament of Sangavar-Zarin Abad. This node also has seismic silence behavior.

Node D17 The nodes are located at the East city of Mianeh and at the intersection of the Sngavar and Masouleh faults. Also, they show the rest seismic behavior.

3.2 Pattern recognition by SOFM

Pattern recognition is a branch of machine learning that focuses on the recognition of patterns and regularities in data, although it is in some cases considered to be nearly synonymous with machine learning. Pattern recognition systems are in many cases trained from labeled "training" data (supervised learning), but when no labeled data are available other algorithms can be used to discover previously unknown patterns (unsupervised learning).

Typically the categories are assumed to be known in advance, although there are techniques to learn the categories (clustering).

In Pattern Recognition applications, many algorithms and models have been proposed for seismology, especially for clustering, regression and classification between earthquakes and explosions. Clustering is defined as unsupervised classification of patterns into groups.

Applications in which a training data set with categories and attributes is available and the goal is to assign a new object to one of a finite number of discrete categories are known as supervised classification problems (Kohonen 1982; Nakamura 2002; Fritzke 1994).

The Self-organizing feature maps (SOFM) defines a mapping from the input data space on to an output layer by the processing units of, e.g., 2-D laminar. Kohonen's algorithm creates a vector quantizer by adjusting weights from common input nodes to M output nodes arranged in a two-dimensional grid as shown in Fig. 3.

Only two-dimensional inputs, like our catalog data, with the weight vectors to unit length have been used. Each neurode in the Kohonen layer receives the input pattern and computes the scalar product of its weight vector with that input vector, in other words, the relative distance between its weight vector and the input vector.

During training, after enough input vectors, weights will specify cluster or vector centers that sample the input space (Dowla et al. 1990).

The Kohonen network models the probability distribution function of the input vectors used during training, with many weight vectors clustering in portions of the hypersphere that have relatively many inputs, and few weight vectors in portions of the hypersphere that have relatively few inputs. The Kohonen networks perform this statistical modeling, even in the cases where no closed-form analytic expression can describe the distribution.

The basic SOFM learning algorithm is to:

1. Choose initial values randomly for all reference vectors.
2. Repeat steps (3), (4), and (5) for discrete time.
3. Perform steps (4) and (5) for each input feature vector.
4. Find the best matching node according to (1).
5. Adjust the feature vectors of all the nodes for each node of the output layer according to:
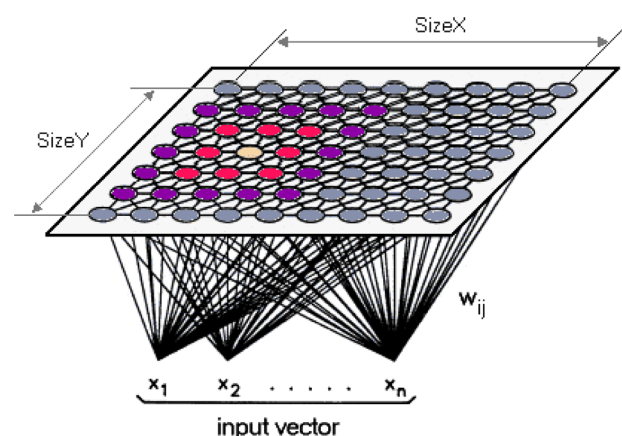
Fig. 3 Two-dimensional array of output data used to form feature maps. The *yellow* neurode is winner neurode and *red* ones are neighborhood neurode

Table 1 Recorded earthquake with magnitude equal or greater than 4.5 in studied area from 1970 until 2015

Date a-mo-d	Time (UTC) h:min:s	Lat. (°N)	Lon. (°E)	Depth (km)	Mag.	Reference
1980-12-19	16:54:18	35.25	52.38	0	M_L:4.5	ISC
1981-08-04	18:53:59	36.45	51.27	0	M_L:4.7	ISC
1982-02-05	23:37:12	36.13	53.68	33	M_L:4.5	ISC
1982-10-25	16:54:50	35.11	52.31	15	M_L:5.4	EHB
1983-03-25	11:57:49	36.04	52.29	20	M_L:5.5	EHB
1983-07-22	02:40:59	36.94	49.22	15	M_L:5.6	EHB
1983-12-20	22:21:04	36.85	50.85	15	M_L:4.8	EHB
1984-09-09	17:55:01	35.53	49.28	49.5	M_L:4.6	ISC
1985-07-08	17:02:35	36.27	53.71	33	M_L:4.7	ISC
1985-10-14	15:28:33	35.58	52.66	15	M_L:4.7	EHB
1986-03-26	15:18:09	36.01	53.68	34.3	M_L:4.6	ISC
1988-08-22	21:23:38	35.32	52.34	22.5	M_L:5.3	EHB
1990-01-20	01:27:12	35.9	52.97	30	M_L:6	EHB
1990-01-20	02:15:07	35.99	53.29	41.6	M_L:4.6	ISC
1990-04-21	21:57:52	36.13	53.1	28.5	M_L:4.5	ISC
1990-06-20	21:00:10	36.99	49.35	18.5	M_L:7.7	ISC
1990-06-20	22:04:07	36.81	49.74	10	M_L:4.7	ISC
1990-06-20	22:23:42	36.99	49.17	10	M_L:5.4	ISC
1990-06-20	22:58:53	36.83	49.47	15	M_L:5.2	EHB
1990-06-20	23:00:39	36.93	49.43	15	M_L:5.2	EHB
1990-06-20	23:27:47	36.89	50.25	33	M_L:5	ISC
1990-06-20	23:48:47	36.71	49.83	15	M_L:5.1	EHB
1990-06-21	00:52:34	36.66	49.67	10	M_L:4.7	ISC
1990-06-21	02:08:53	36.79	49.76	15.5	M_L:5.4	EHB
1990-06-21	07:50:25	36.86	49.48	15	M_L:4.9	EHB
1990-06-21	09:02:16	36.63	49.79	13.6	M_L:5.8	EHB
1990-06-21	12:17:30	36.87	49.45	15	M_L:5.1	EHB
1990-06-21	21:27:41	36.58	49.69	10	M_L:4.8	EHB
1990-06-21	21:31:10	36.76	49.35	15	M_L:4.7	EHB
1990-06-22	06:21:52	36.62	49.44	10	M_L:4.7	ISC
1990-06-24	09:45:59	36.84	49.41	15	M_L:5.3	EHB
1990-06-24	19:05:24	37	49.59	33	M_L:4.6	ISC
1990-06-27	03:56:23	36.87	49.71	20	M_L:4.9	EHB
1990-06-28	03:20:38	36.87	49.52	20	M_L:4.8	EHB
1990-06-28	17:21:07	36.77	49.87	20	M_L:4.7	EHB
1990-06-29	06:25:51	36.67	49.91	46	M_L:4.5	ISC
1990-07-06	19:34:52	36.86	49.3	20	M_L:5.3	EHB
1990-07-13	13:04:11	36.8	50.11	33	M_L:4.7	ISC
1990-08-13	06:18:24	36.71	49.89	15	M_L:4.6	EHB
1990-08-20	12:20:11	36.8	49.63	15	M_L:4.7	EHB
1990-08-21	03:47:28	36.95	49.49	15	M_L:4.8	EHB
1990-09-25	12:12:18	36.69	49.77	15	M_L:4.9	EHB
1990-10-17	17:06:29	36.88	49.49	15	M_L:4.5	EHB
1990-10-22	03:50:24	36.91	49.39	25	M_L:4.7	EHB
1990-12-27	13:26:57	36.94	49.24	10.1	M_L:4.7	EHB
1990-12-28	04:03:55	36.96	49.2	15	M_L:5	EHB
1991-01-22	12:04:25	35.44	52.32	33	M_L:4.5	ISC
1991-05-29	15:15:21	36.23	53.24	33.1	M_L:4.5	ISC
1991-08-23	22:14:21	35.99	53.27	42	M_L:5	ISC

Table 1 continued

Date a-mo-d	Time (UTC) h:min:s	Lat. (°N)	Lon. (°E)	Depth (km)	Mag.	Reference
1991-11-28	17:19:56	36.83	49.58	15	M_L:5.6	EHB
1991-12-18	16:42:21	36.53	49.69	15	M_L:4.6	EHB
1992-09-22	14:05:56	36.29	52.72	35	M_L:5.1	EHB
1993-06-30	23:05:37	35.17	53.56	25	M_L:4.6	EHB
1993-08-19	10:04:30	35.17	52.1	16.3	M_L:4.6	EHB
1993-10-18	01:28:24	36.55	53.78	33	M_L:4.5	ISC
1994-11-21	18:55:18	36.05	51.91	43.9	M_L:4.5	ISC
1995-04-26	11:46:11	36.93	49.4	15	M_L:4.6	EHB
1998-01-09	19:06:13	36.38	52.15	15	M_L:4.6	EHB
1998-04-04	02:46:31	36.61	49.52	16.7	M_L:4.5	ISC
1999-12-09	22:20:37	36.45	53.57	15	M_L:4.5	EHB
2002-04-08	18:30:55	36.42	51.99	8.5	M_L:4.8	EHB
2002-04-19	13:46:51	36.52	49.75	28.5	M_L:5.2	EHB
2002-06-22	02:58:23	35.6	49.02	11	M_L:6.5	EHB
2002-10-10	12:13:43	35.89	52.33	33	M_L:4.7	NEIC
2003-06-21	15:00:05	35.63	52.86	23.9	M_L:4.5	ISC
2003-12-24	03:50:00	35.17	50.5	15	M_L:4.7	EHB
2004-05-28	12:38:45	36.26	51.57	26.7	M_L:6.4	EHB
2004-05-28	13:15:07	36.44	51.59	37	M_L:4.6	IIEES
2004-05-28	19:47:05	36.43	51.4	25	M_L:4.5	EHB
2004-05-29	09:23:49	36.49	51.4	14.2	M_L:4.7	EHB
2004-05-29	18:38:07	36.45	51.37	28	M_L:4.6	IIEES
2004-05-30	01:42:41	36.4	51.61	28	M_L:4.5	IIEES
2008-03-26	18:49:55	36.25	52.73	14.1	M_L:4.5	IIEES
2012-01-11	17:08:00	36.37	52.83	16.4	M_L:5.2	IIEES
2012-02-10	08:59:40	35.59	52.42	14.3	M_L:4.6	IIEES
2012-03-18	02:38:16	36.82	49.2	14.1	M_L:4.5	IIEES
2013-03-21	19:37:04	36.19	53.69	14.1	M_L:4.8	IIEES
2013-10-16	08:49:32	35.29	49.73	6.1	M_L:4.6	IIEES

$$w_{ia}(t+1) = w_{ia}(t) + \eta(t)[x_i(t) - w_{ia}(t)].$$

where $\eta(t)$ is learning rate. It starts with an initial value η_0 and decrease with time but it never reach 0.

Repeat this procedure until convergence, e.g., until the error between the input data and the corresponding neuron representing their class falls below a certain threshold.

When the network converges to its final stable state following a successful learning process, it displays three major properties:

1. The SFOM map is a good approximation to the input sample space. This property is important since it provides a concentration of representation of the given input space.
2. The feature map naturally forms a topologically ordered output space such that the spatial location of a neuron in the lattice corresponds to a particular domain in input space.
3. The feature map embodies a statistical law. In other words, the input with more frequent occurrence occupies a larger output domain of the output space.

This property helps to make the SOFM an optimum codebook of the given input space.

The straightforward way to take advantage of the above properties for prediction is to create SOFM from the input vector, since such a feature map provides a faithful topologically organized output of the input vectors.

If the input pattern is allowed to be in any unusual pattern or distribution, the Kohonen network will always generate a map of that distribution. These plots look a little like a topological map of a hilly region. Where many input vectors are clustered, the grid is similarly bunched and
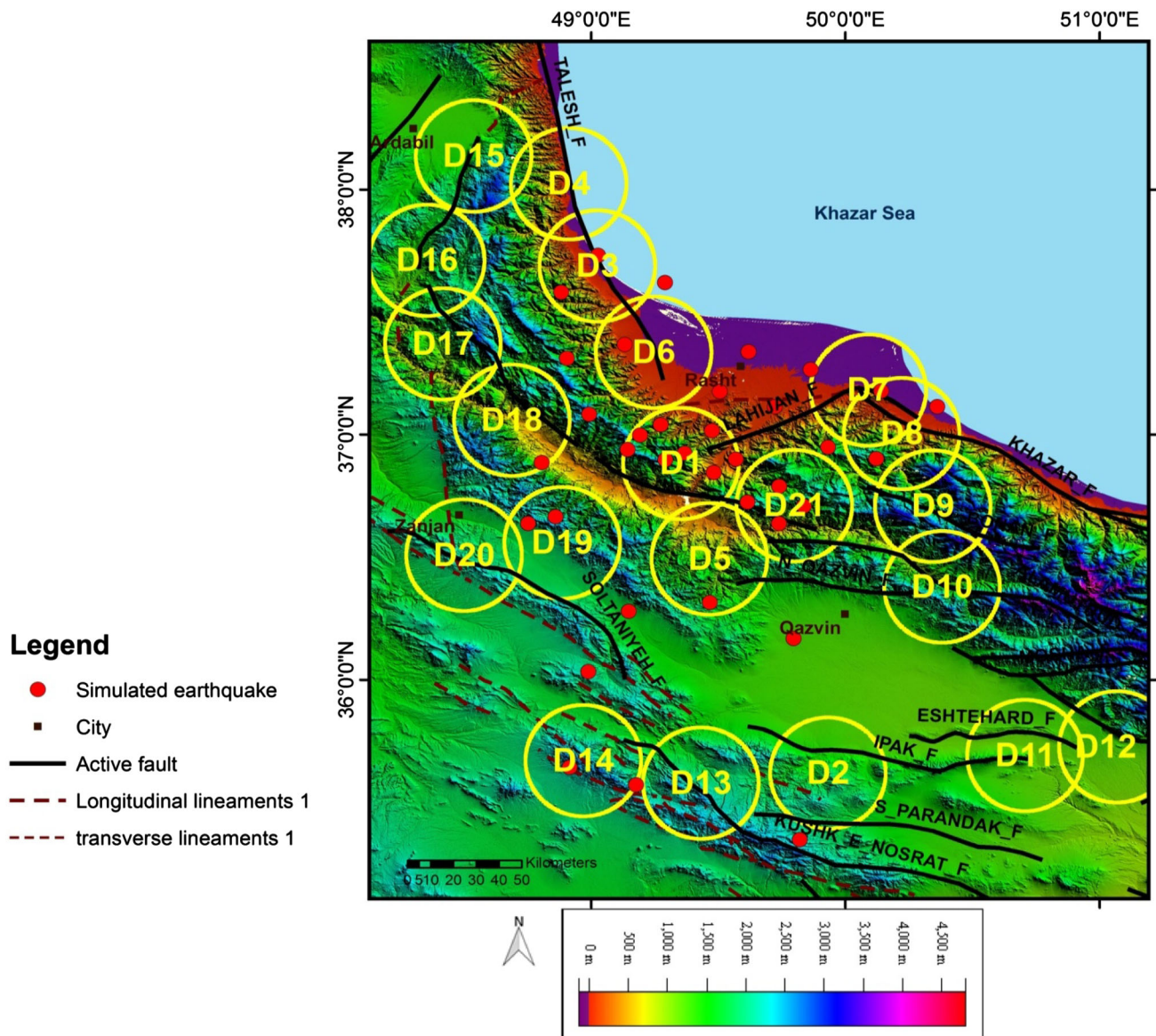
Fig. 4 Simulated earthquakes. The *red points* are next big events

crowded. Where only a few input vectors are clustered, the grid is much sparser. In this work, input sample space is latitude and longitude of earthquakes from 1980 to 2015 and the discrete output space, respectively, are 9×9 neurons that receive input from the previous layer and generate output to the next layer or outside world.

After data mining nodes in the Western Alborz by using the mentioned method, the self-organized neural networks use for determining the approximate next event place and the relative comparison between the tectonic activity levels nodes, and also, evaluate the inside scope of any node by Pattern Recognition method.

Using this method, in addition to identifying hazardous areas, is in acceptance with MZ method. Similarly, it can

be seen the predicted nucleation of next earthquakes is more formed around nodes.

4 Conclusions

The SOFM algorithm is renowned as one of the most elegant competitive learning networks ever designed. Unlike supervised neural network systems, the Kohonen SOFM "acquires the ability" to classify nonlinear datasets. The SOFM acts to "self-organize" and systematically minimize the Euclidean distance among input values, producing a constellation of best fit data patterns. That is given that a set of unambiguous patterns may exist within a

given chaotic nonlinear dataset, the SOFM algorithm isolates and numerically classifies seismic nonlinear patterns that form a visually conspicuous earthquakes cluster of output values. The SOFM can capture underlying data patterns and provide illustrative displays of crucial dimensions and characteristics of a given catalog makes this algorithm a particularly important tool when conducting any form of data catalog distinguish it from classical multivariate statistical methodologies for earthquake forecasting.

By considering historical and instrumental earthquake catalogs with clear magnitudes, high-risk seismic nodes identified. Our used inputs in SOFM were longitude and latitude of recorded earthquakes greater than 4.5 magnitude (Table 1).

The simulated point by using SOFM in Fig. 4 forecasts the future big earthquakes.

As is shown in Fig. 4, 36 simulated events have located on the map as future earthquakes with magnitude greater than 5.5 located on the map. Among all nodes, node D1 has most number of points (almost 7 events), also donut shapes, constituted of events in this node, can be seen, so that it is determined as highest potential risk region. It was expectative that this node is located on the Rudbar fault, with the biggest destructive earthquake in past.

Node D21, within 4 large earthquakes, determined as next hazardous node. One of the points stands on the borders of D7 and D14. They all are considered as same seismicity potential risk together.

Some seismic node patterns near in the middle of Lahijan fault, between D1 and D7 nodes, have high seismicity potential risk (meet seismic quiescence) that can be introduced as a new hazardous node.

Nearly, 70% of simulated events has stand in the seismic nodes or on their boundaries. So it can be observed that simulated earthquakes by neural network are in acceptance with the ideas of MZ method to determine high-seismic-risk regions.

References

Alexeevskaya MA, Gabrielov AM, Gvishiani AD, Gelfand IM, Rantsman E Ya (1977) Formal morphostructural zoning of mountain territories. J Geophys Res 43:227–233

Assameur DM, Mareschal JC (1995) Stress induced by topography and crustal density heterogeneities; implication for the seismicity of southeastern Canada. Tectonophysics 241:179–192

Berberian M (1983) The southern Caspian: a compressional depression floored by a trapped, modified oceanic crust. Can J Earth Sci 20(2):163–183

Berberian M, Walker R (2010) The Rudbar Mw 7.3 earthquake of, 1990 June 20; seismotectonics coseismic and geomorphic displacements and historic earthquakes of the western 'High-Alborz', Iran. Geophys J Int 182(3):1577–1602

Berberian M, Yeats RS (2001) Contribution of archaeological data to studies of earthquake history in the Iranian Plateau. Paul Hancock memorial issue. J Struct Geol 23:536–584

Bott MHP, Dean DS (1972) Stress systems at younger continental margins. Nature 235:23–25

Dalmayrac B, Molnar P (1981) Parallel thrust and normal faulting in peru and constraints on the state of stress. Earth Planet Sci Lett 55:473–481

Dowla FU, Taylor SR, Anderson RW (1990) Seismic discrimination with artificial neural networks: preliminary results with regional spectral data. Bull Seism Soc Am 80:1910–1933

England P, McKenzie DP (1982) A thin viscous sheet model for continental deformation. Geophys J R Astron Soc 70:295–321

Fritzke B (1994) Growing cell structures-H self-organizing network for unsupervised and supervised learning. Neural Netw 7(9):1141–1160

Gelfand I, Graev MI, Shapiro Z Ya (1970) The classification of the linear representation of the group SL (2, C). Dokl Akad Nauk SSSR 194:1002–1005

Gelfand I, Guberman Sh, Izvekova M, Keilis-Borok V, Rantsman E (1972) Criteria of high seismicity, determined by pattern recognition. Tectonophysics 13:415–422

Geller J (1997) Earthquake prediction: a critical review. Geophysicak J Int 131(3):425–450

Gheitanchi MR, Mirzaei N, Sadikkhoy A (2006) Seismic activity in Alborz, northern Iran, revealed by local seismic network. Geoscience 58:191

Gorshkov AI, Gaudemer Y (2012) Identification of seismogenic nodes in an area of low seismicity (case of the Massif Central, France). Book of Abstracts of the 33rd General Assembly of the European Seismological Commission. 19–24 August 2012. Moscow, 380

Gorshkov AI, Panza GF, Soloviev AA, Aoudia A (2002) Morphostructural zonation and preliminary recognition of seismogenic nodes around the Adria margin in peninsular Italy and Sicily. J Seismol Earthq Eng 4(1):1–24

Gorshkov A, Kossobokov V, Soloviev A (2003) Recognition of earthquake-prone areas. Springer, Heidelberg, pp 239–310

Gorshkov AI, Panza GF, Soloviev AA, Aoudia A (2004) Identification of seismogenic nodes in the Alps and Dinarides. Bollettino della Società geologica italiana 123(1):3–18

Gorshkov AI, Mokhtari M, Piotrovskaya EP (2009) The Alborz region: identification of seismogenic nodes with morphostructural zoning and pattern recognition. J Seismol Earthq Eng 11(1):1–15

Gorshkov AI, Soloviev AA, Jiménez MJ, García-Fernández M, Panza GF (2010) Recognition of earthquake-prone areas (M ≥ 5.0) in the Iberian Peninsula. Rendiconti Lincei-Scienze Fisiche e Naturali 21(2):131–162

Hessami Kh, Jamali F, Tabassi H (2003) Major Active Faults of Iran. IIEES

Jackson J (1992) Partitioning of strike-slip and convergent motion between Eurasia and Arabia in eastern Turkey and the Caucasus. J Geophys Res 97:12471–12479

Jackson JA, McKenzie DP (1984) Active tectonics of the Alpine-Himalayan belt between western Turkey and Pakistan. Geophys J R Astron Soc 77:185–264

Jackson D, Kagan Y, Wang Qi (2009) California earthquakes 1800–2007: a unified catalog with moment magnitudes, uncertainties, and focal mechanisms. Seismol Res Lett l 80(3):446–457

Jordan T, Chen Y, Gasparini P, Madariaga R, Main I, Marzocchi W, Papadopoulos G, Sobolev G, Yamaoka K, Zschau J (2011) ICEF Report. Operational earthquake forecasting: state of knowledge and guidelines for utilization. Ann Geophys 54(4):315–391

Kagan Y, Shen Zheng-Kang, Jackson D (2007) Implications of geodetic strain rate for future earthquakes, with a five-year forecast of M5 earthquakes in southern California. Seismol Res Lett 78(1):116–120

Keary P, Vine FJ (1996) Global Tectonics. Blackwell Scientific Publications, London, p 302

Keilis-Borok VI (1990) The lithosphere of the Earth as a nonlinear system with implications for earthquake prediction. Rev Geophys 28:19–34

Kohonen T (1982) Self-organized formation of topologically correct feature maps. Biol Cybern 43:59–69

Moores EM, Twiss RJ (1995) Tectonics. Freeman, New York, p 415

Nakamura AA (2002) P-wave velocity structure of the crust and its relationship to occurrence of the 1999 Izmit, Turkey earthquake and aftershocks. Bull Seismol Soc Am 92(1):330–338

Nogol Sadat MAA (1978) Les zone de decrochement et les virgations structurales en Iran. Concequences des resultants de lanalyse renoblel de la reigon de qom. These Univ. Scientifique et Medicate de renoble, 201

Peresan A, Zuccolo E, Vaccari F, Gorshkov A, Panza GF (2011) Neo-deterministic seismic hazard and pattern recognition techniques: time dependent scenarios for North-Eastern Italy. Pure Appl Geophys 168(3–4):583–607

Peresan A, Magrin A, Vaccari F, Panza GF (2013) Prospective testing of time-dependent neodeterministic seismic hazard scenarios. In: Proceedings of the 31st GNDT Convegno del Gruppo Nazionale di Geofisica della Terra Solida (Potenza, 20–22 November 2012), pp 429–433

Reyes J, Morales-Estebanb A, Martnez-Alvarez F (2012) Neural networks to predict earthquakes in Chile. Appl Soft Comput 13:1314–1328

Seeber L, Armbruster JG, Quittmeyer RC (1981) Seismicity and continental subduction in the Himalayan Arc. In: Gupta HK, Delany FM (eds.) Zagros Hindu Kush Himalaya Geodynamic Evolution. Geodynamic Series 3, Am Geophy Union Washington, DC and Geological Society of America, Boulder, CO, 215–242

Snyder DB, Barazangi M (1986) Deep crustal structure and flexure of the Arabiyan plate beneath the zagros collisional mountain belt as inferred from gravity observations. Tectonics 5:361–373

Soloviev AA, Gvishiani AD, Gorshkov AI, Dobrovolsky MN, Novikova OV (2014) Recognition of earthquake-prone areas: methodology and analysis of the results. Izvestiya Phys Solid Earth 50(2):151–168

Talwani P (1988) The intersection model for intraplate earthquakes. Seismol Res Lett 59(4):305–310

Tiampo KF, Shcherbakov R (2012) Seismicity-based earthquake forecasting techniques: ten years of progress. Tectonophysics 522–523:89–121

Ward S (2000) San Francisco Bay Area earthquake simulations: A step toward a standard physical earthquake model. Bulletin of the Seismological Society of America, Institute of Tectonics, University of California, Santa Cruz, CA 95064

Ward S (2007) Methods for evaluating earthquake potential and likelihood in and around California. Seismol Res Lett 78(1):121–133

Zamani A, Hashemi N (2000) A Comparison between seismicity, topographic relief, and gravity anomalies of the Iranian Plateau. Tectonophysics 327:25–36

Zolfaghari MR (2008) GPS-measured slip rates vs. seismic moment released by past seismicity alone Alborz mountain rang in Iran. In: The 14th World Conference on Earthquake Engineering October 12–17, 2008, Beijing, China